

**Contract No:**

This document was prepared in conjunction with work accomplished under Contract No. DE-AC09-09SR22505 with the U.S. Department of Energy (DOE) National Nuclear Security Administration (NA).

**Disclaimer:**

This work was prepared under an agreement with and funded by the U.S. Government. Neither the U.S. Government or its employees, nor any of its contractors, subcontractors or their employees, makes any express or implied:

- 1) warranty or assumes any legal liability for the accuracy, completeness, or for the use or results of such use of any information, product, or process disclosed; or
- 2) representation that such use or results of such use would not infringe privately owned rights; or
- 3) endorsement or recommendation of any specifically identified commercial product, process, or service.

Any views and opinions of authors expressed in this work do not necessarily state or reflect those of the United States Government, or its contractors, or subcontractors.

## **Use of Regression Analysis to Abstract a Complex Percolation Model into a Simplified Site-Specific Empirical Formula – 22126**

Steve Hommel  
Savannah River Remediation

### **ABSTRACT**

The Performance Assessment (PA) for the Saltstone Disposal Facility (SDF) at the Savannah River Site (SRS) used a variably saturated flow model to estimate surface conditions and annual percolation through a closure cap that will be placed over the SDF after closure. The estimated annual percolation was used to define the water flux into the top boundary of vadose zone flow models used to simulate the near field conditions. The need arose to develop a more dynamic approach for estimating these water fluxes under variable conditions based on specific independent variables, such as precipitation and surface erosion. However, the variably saturated flow models used to simulate the closure cap conditions are complex and do not support the probabilistic simulations necessary for applying variable conditions. To overcome this challenge, a series of deterministic simulations were developed by modifying the variably saturated flow model to use specific values for the precipitation and the depth of surface erosion. This series of deterministic simulations provided a sample set of percolations based on the given inputs. Next, regression analyses were performed to develop a site-specific empirical formula for estimating percolation based on precipitation and erosional depth. Finally, the site-specific empirical formula was applied to a fully probabilistic closure cap model to generate a complete range of potential water fluxes into the vadose zone. This approach may be applied to other complex models with multiple independent variables to develop more efficient probabilistic system models.

### **INTRODUCTION**

The SRS Liquid Waste System (LWS) safely stores and treats liquid radioactive waste. The LWS consists of 51 waste storage tanks (eight of which are operationally closed and filled with grout), waste evaporators, treatment facilities, and solidification facilities such as the Defense Waste Processing Facility (DWPF) and Saltstone Production Facility (SPF). The tank farms at SRS have received over  $6.06\text{E}+08$  L (160 Mgal) of radioactive waste since 1954. [1] The liquid waste will be dispositioned as either low-level waste (destined for the SDF via the SPF) or high-level waste (destined for a federal repository via the DWPF).

The soluble waste from the tank farms undergoes a decontamination process to remove cesium and other high-activity constituents. After decontamination, the low-activity salt solution is sent to the SPF where it is used to produce a grout slurry. The grout slurry is then pumped into Saltstone Disposal Units (SDUs) where it cures (or hardens) into the final low-level wasteform called saltstone. [1] This wasteform has been designed to immobilize radionuclides and chemicals.

Saltstone production began in June 1990 and has continued until present day. The SDUs currently containing saltstone are SDUs 1, 2A, 2B, 3A, 4, 5A, 5B, and 6. [2] In support of continued waste disposal operations at the SDF, additional SDUs will be constructed and filled with saltstone. [1] Once disposal operations end, the SDF will be prepared for permanent closure. [3] As part of SDF closure, a permanent engineered closure cap will be installed over the SDUs. This closure cap will consist of multiple layers of both engineered and earthen materials to prevent or limit water ingress to the SDUs.

*The Performance Assessment for the Saltstone Disposal Facility at the Savannah River Site* [4] (hereafter referred to as the SDF PA) was issued in March 2020 to inform decisions regarding waste disposal operations and closure and to demonstrate that the SDF system will meet the requirements of the U.S.

Department of Energy's (DOE) Manual 435.1-1, *Radioactive Waste Management Manual*. [5]

In October 2020, the U. S. Nuclear Regulatory Commission (NRC) issued a letter [6] which included Requests for Supplemental Information (RSIs) to support their review of the SDF PA. Responses to a number of the RSIs required sequential analyses, resulting in multiple RSI-response documents being prepared from March 2021 to August 2021. [7] The site-specific empirical formula discussed herein was developed in support of the response to "RSI-1: Combined Uncertainty of Flow Barriers." [8]

### SDF Facility Overview

The SDF currently consists of two 183 m (600 ft) long rectangular SDUs (Figure 1, SDUs 1 and 4), three pairs of 46 m (150 ft) diameter SDUs (Figure 1, SDUs 2 A/B, 3 A/B, and 5 A/B), and four 114 m (375 ft) diameter SDUs (Figure 1, SDUs 6, 7, 8, and 9). Note that SDUs 8 and 9 are still in various stages of construction and are not yet operational. The final layout for the SDF will include a total of seven 114 m (375 ft) diameter SDUs. By the time of facility closure, the SDF will consist of 15 SDUs with a combined capacity of over  $1.06\text{E}+09$  L (280 Mgal) of cured saltstone. [4]

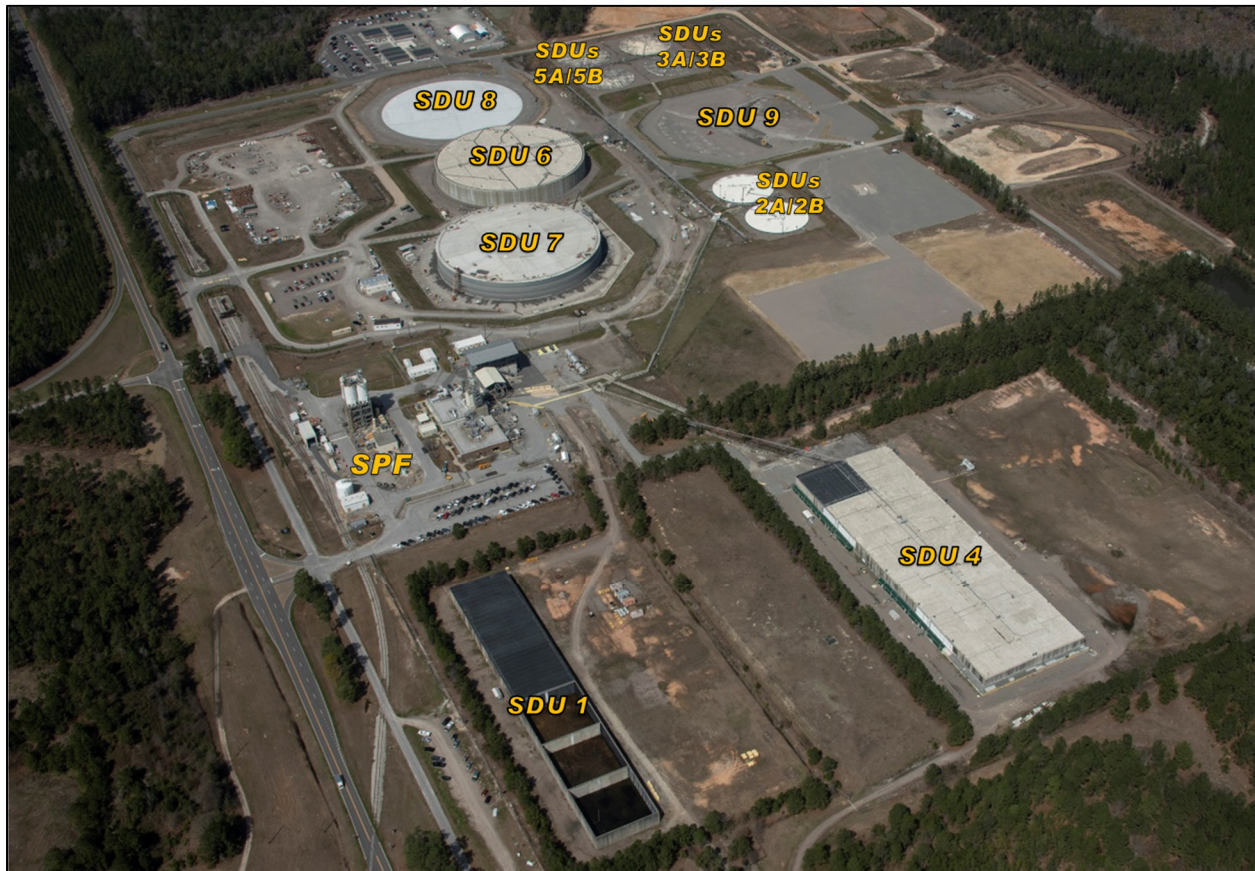
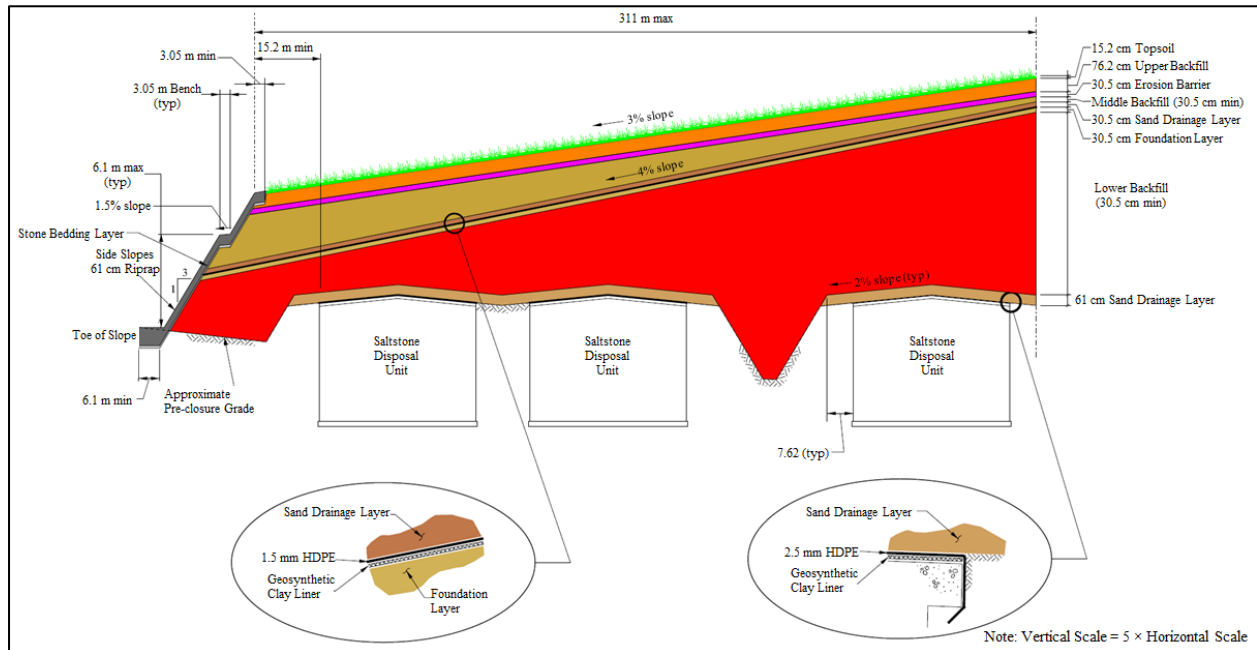


Fig. 1. Saltstone Disposal Facility at SRS.

### SDF Closure Cap Design

The layers and materials of the current SDF closure cap design are based on *Saltstone Disposal Facility Closure Cap Concept and Infiltration Estimates* [9], while the geometry and the layout of the closure cap have been updated to accommodate larger SDUs. [10] The updated geometry also incorporates an increased slope at the surface (i.e., 3% slope instead of 1.5% slope) to meet closure requirements

The SDF closure cap is primarily intended to provide physical stabilization of the site, minimize infiltration, and provide an intruder deterrent. Figure 2 shows a typical cross section from this conceptual closure cap design. [10] Table I specifies each of the SDF closure cap layers and their anticipated thicknesses. [9]



### RSI-1: Combined Uncertainty of Flow Barriers

In their October 2020 letter [6], NRC staff identified eight RSIs. For the first RSI (RSI-1), the NRC staff requested additional information about the combined uncertainties of the multiple flow barriers used to prevent or limit the ingress of water into the SDUs. As part of this request, the NRC also proposed a recommended path forward:

3

To respond to RSI-1, other RSIs had to be addressed first. RSI-2 and RSI-3 requested a detailed evaluation of uncertainties related to the performance of the sand drainage layers, the HDPE, and the GCL within the SDF closure cap, while RSI-7 requested an evaluation of uncertainties related to erosion. [6] Once these prerequisite RSIs were addressed [12, 13, 14], a fully probabilistic closure cap model was needed to provide an in-depth evaluation of uncertainties associated with the closure cap and to generate probabilistic water fluxes for use in the vadose zone models prepared in response to RSI-1. [8]

TABLE I. SDF Closure Cap Layers and Layer Thicknesses

Layer <sup>a</sup>	Layer Thickness (cm)	Layer Thickness (in)
Vegetative Cover	N/A	N/A
Topsoil	15.2	6
Upper Backfill	76.2	30
Erosion Barrier	30.5	12
Geotextile Fabric	N/A	N/A
Middle Backfill	30.5 (minimum) <sup>b</sup>	12 (minimum) <sup>b</sup>
Geotextile Filter Fabric	0.25 (minimum)	0.1 (minimum)
Upper Lateral Sand Drainage Layer	30.5	12
Geotextile Fabric	N/A	N/A
High Density Polyethylene (HDPE) Geomembrane	0.15	0.06
Geosynthetic Clay Liner (GCL)	0.5	0.2
Foundation Layer (backfill with bentonite admix)	30.5	12
Lower Backfill	30.5 (minimum) <sup>c</sup>	12 (minimum) <sup>c</sup>

**Footnotes:**

N/A = Not available or not applicable.

<sup>a</sup> The layers are arranged in the table to reflect their order from top to bottom in the SDF closure cap.

<sup>b</sup> Thickness will increase from closure cap apex to closure cap edge due to difference between surface slope and the slope of the upper lateral sand drainage layer.

<sup>c</sup> Thickness will decrease from closure cap apex to closure cap edge due to the slope of the upper lateral sand drainage layer.

**DESCRIPTION**

Conceptually, the SDF closure cap modeling for the SDF PA was organized into two parts. The first part, hereafter referred to as the “Percolation Model”, estimated the percolation through the upper layers of the closure cap down to the upper lateral drainage layer (Figure 3), while the second part estimated the leakage rate through the “composite barrier” (i.e., the combined HDPE and GCL layers) below the upper lateral sand drainage layer. This leakage rate was then applied as a water flux input for vadose zone flow models that begin at the top of the lower backfill layer and extend down through the subsurface to the top of the water table beneath each of the SDUs.

The Percolation Model (Figure 3) applied meteorological and environmental conditions and material properties that influence percolation through the upper lateral sand drainage layer. As shown, water is introduced into the system as precipitation (P). Solar radiation and vegetation remove water from the system via evaporation (E) and transpiration (T), respectively. Surface runoff (R) also removes water from the system. The remaining water is then expected to percolate downward past the root zone. The rate of percolation (Pr) is affected by the hydraulic properties and thicknesses of each layer of the closure cap through the upper lateral sand drainage layer.

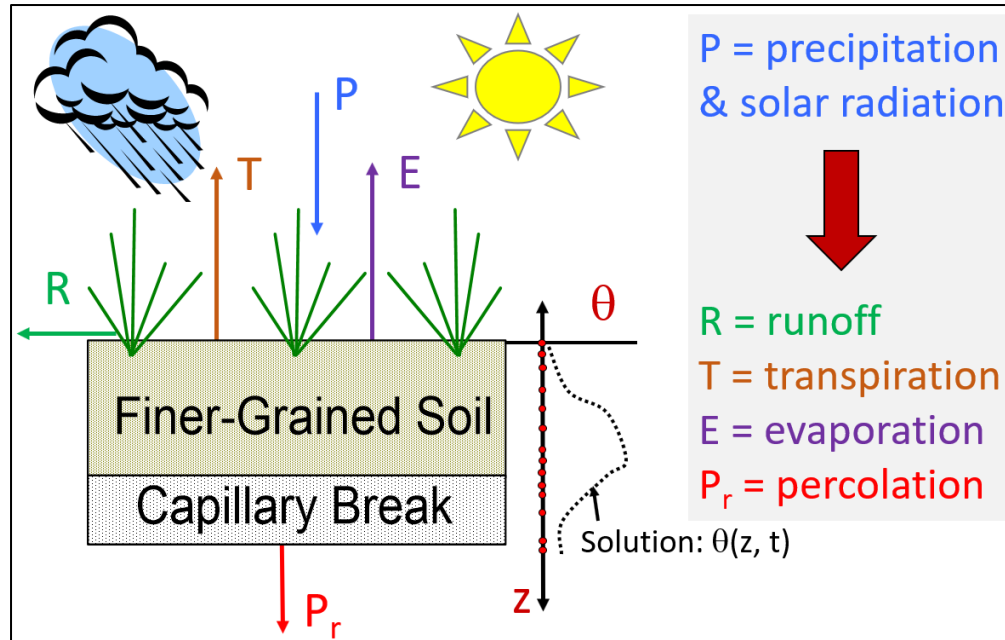


Fig. 3. Conceptual Model for Percolation Through the Upper Closure Cap.

This Percolation Model was performed using a software designed for complex water balance equations (UNSAT-H) to simulate the variably saturated flow conditions based on a set of pre-defined environmental conditions and material properties. Within the SDF PA, this Percolation Model estimated annual percolation of approximately 400 mm based on expected conditions. [4]

#### Uncertainty in the Long-Term Precipitation at SRS

Figure 4 shows the annual precipitation at SRS from 1960 through 2020 based on data collected from multiple SRS weather stations. This figure shows the annual mean across all SRS stations and also the annual mean for all the years: a value of 1,255 mm (49.4 inches). Collectively, the data from these weather stations provides 583 data points for annual precipitation at SRS, with a minimum value of 729 mm (28.7 inches) and a maximum value of 1,991 mm (78.4 inches). [14]

An analysis of the regional paleoclimate was also performed. From that analysis, it was determined that the frequency of major changes to the climate was on the order of  $1.01\text{E-}04/\text{yr}$  (i.e., approximately one major climate transition for every 10,000 years). [14] No conclusions could be drawn regarding whether the next climate transition at SRS would result in a drier or wetter climate; however, it was determined that if a drier climate occurs, annual precipitation would likely decrease by approximately 25% while a wetter climate would likely see annual precipitation increase by approximately 25%. [14]



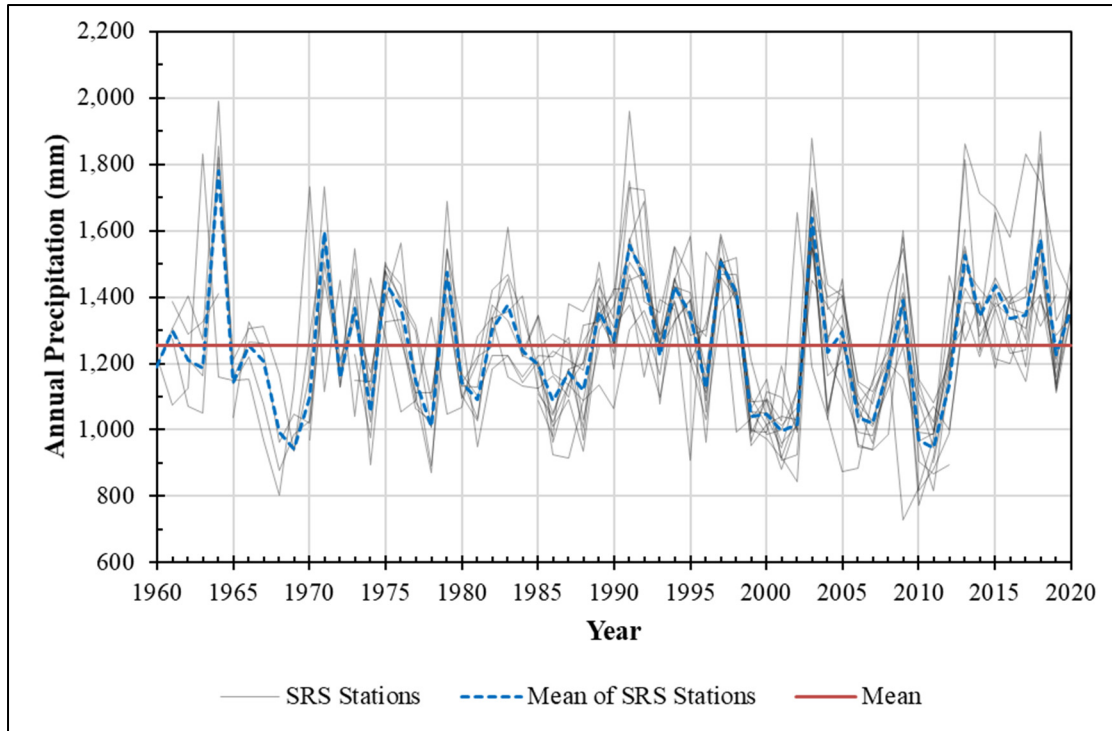


Fig. 4. Annual Precipitation at SRS from 1960 through 2020.

### Uncertainty in Closure Cap Erosion Rates

From the surface of the closure cap, Table I showed the top of the erosion barrier at a depth of 91.4 cm (3 feet). It is assumed that the erosion barrier will be constructed from large rocks or engineered materials designed to be resistant to erosion. However, the material above the erosion barrier might be subjected to some amount of surface or sheet erosion over the long periods considered in the SDF PA. Using the Revised Universal Soil Loss Equation (RUSLE) from the U. S. Department of Agriculture (USDA) [15], the rate of potential soil loss can be estimated and used to evaluate erosion as a function of precipitation and other variables (e.g., vegetative cover, soil density, and the soil erodibility factor). [14] From this analysis, it was determined that the depth of surface erosion may vary over time from 0 cm (no erosion) to 91.4 cm (for complete erosion down to the erosion barrier).

### Challenge in Applying these Uncertainties to Probabilistic Modeling

For the SDF PA, the Percolation Model assumed long-term environmental conditions would be similar to current conditions. This modeling simplification was adopted because each input parameter in the Percolation Model requires a single pre-defined value (i.e., the Percolation Model does not support dynamic sampling of statistical distributions or changes to the system features over time).

While this static approach used for the SDF PA offers a reasonable estimate of annual percolation and water balance evolution [8], an alternative approach must be adopted to address the probabilistic uncertainties raised by the NRC's RSI-1. Specifically, in order to fully address uncertainties in percolation, a model would need to be able to sample the annual precipitation, then apply the sampled precipitation value to the RUSLE formula to estimate annual erosion, then apply both the sampled precipitation value and the estimated material thicknesses (after erosion) to the Percolation Model. The Percolation Model would then need to be re-run for every realization and every time step any time either the precipitation value or the material thicknesses changed. Since the Percolation Model can take several

hours to run and only provides results for one year at a time, this approach would be extremely inefficient.

### Alternative Approach to Support Probabilistic Modeling

The alternative approach was to develop and apply an empirical formula that could approximate the site-specific results from the Percolation Model. The empirical formula could be developed such that percolation may be estimated from both sampled annual precipitation and changing erosional depths.

To develop this empirical formula, a series of deterministic simulations were prepared by modifying the Percolation Model to use specific values for both the annual precipitation and the erosional depth of the soil. This series of deterministic simulations provided a sample set of estimated percolations. Next, regression analyses were used to generate line-fitting equations for percolation as a function of precipitation and erosional depth. These simple line-fit equations can then be used in lieu of the more complex Percolation Model.

### DISCUSSION

The annual precipitation (Figure 4) varies along a normal distribution with a mean of 1,255 mm and standard deviation of 217 mm. A standalone probabilistic model was developed to sample values with this distribution to provide additional insights with respect to variability in the system. Climate change was applied within this standalone model by multiplying the sampled precipitation values by factor of 0.75 (for drier climates) or 1.25 (for wetter climates). These distributions were sampled 1,000 times. Table II shows a summary of sampled precipitation values based on these conditions.

TABLE II. Sampled Annual Precipitation for SDF Modeling

Selected Percentiles	Annual Precipitation (mm)		
	Assumed Drier Climate Condition <sup>a</sup>	Current Climate Condition	Assumed Wetter Climate Condition <sup>a</sup>
100%	1,374	1,969	2,461
90%	1,140	1,532	1,935
50%	935	1,257	1,582
10%	747	986	1,214
0%	554	739	930

#### Footnotes:

<sup>a</sup> These assumed climate condition values represent a summary of model results from a standalone probabilistic model and may not exactly match the value from the Current Climate Condition column multiplied by the respective climate change multiplier (0.75 for the drier climate and 1.25 for the wetter climate).

The 10<sup>th</sup>, 50<sup>th</sup>, and 90<sup>th</sup> percentile values (representing assumed low, intermediate, and high precipitation values) from each of the climate conditions (drier, current, or wetter) were each used as inputs to a set of percolation models. Each of the nine percolation models were re-run four times (for a total of 36 percolation models) using a different depth of erosion (0 cm, 30.5 cm, 61.0 cm, or 91.4 cm) each time. The selected erosion depths represent no erosion (0 cm), complete erosion down to the erosion barrier of the closure cap (91.4 cm), and two intermediate values. The estimated annual percolation from each of these modeling cases are provided in Table III. The estimated annual percolation ranged from 63.5 mm (for the case with the low precipitation, a drier climate, and complete erosion) to 782 mm (for the case with the high precipitation, a wetter climate, and no erosion). [8]

Next, the percolation result from each of the modeling cases were plotted against the corresponding soil thicknesses and trendlines were added to connect results from modeling cases with the same precipitation



inputs (Figure 5). This analysis revealed that as the thickness of the soil above the erosion barrier approaches 0 cm, the percolation rates decreased. [8] This is largely because runoff and evaporation rates increased under these conditions. [16]

TABLE III. Estimated Percolation (mm) from Each of the Percolation Models

<b>Simulation ID</b>	<b>Precipitation (mm)</b>	<b>Erosion Depth (cm)</b>	<b>Percolation (mm)</b>
HW Thk91.4	1,935	0.0	784
HW Thk61.0	1,935	30.5	730
HW Thk30.5	1,935	61.0	631
HW Thk0.0	1,935	91.4	303
HC Thk91.4	1,532	0.0	524
HC Thk61.0	1,532	30.5	504
HC Thk30.5	1,532	61.0	454
HC Thk0.0	1,532	91.4	227
HD Thk91.4	1,140	0.0	311
HD Thk61.0	1,140	30.5	308
HD Thk30.5	1,140	61.0	282
HD Thk0.0	1,140	91.4	158
IW Thk91.4	1,582	0.0	557
IW Thk61.0	1,582	30.5	533
IW Thk30.5	1,582	61.0	478
IW Thk0.0	1,582	91.4	238
IC Thk91.4	1,257	0.0	386
IC Thk61.0	1,257	30.5	373
IC Thk30.5	1,257	61.0	340
IC Thk0.0	1,257	91.4	182
ID Thk91.4	935	0.0	163
ID Thk61.0	935	30.5	159
ID Thk30.5	935	61.0	158
ID Thk0.0	935	91.4	122
LW Thk91.4	1,214	0.0	358
LW Thk61.0	1,214	30.5	350
LW Thk30.5	1,214	61.0	319
LW Thk0.0	1,214	91.4	173
LC Thk91.4	986	0.0	185
LC Thk61.0	986	30.5	183
LC Thk30.5	986	61.0	183
LC Thk0.0	986	91.4	118
LD Thk91.4	747	0.0	108
LD Thk61.0	747	30.5	97.9
LD Thk30.5	747	61.0	89.0
LD Thk0.0	747	91.4	62.3

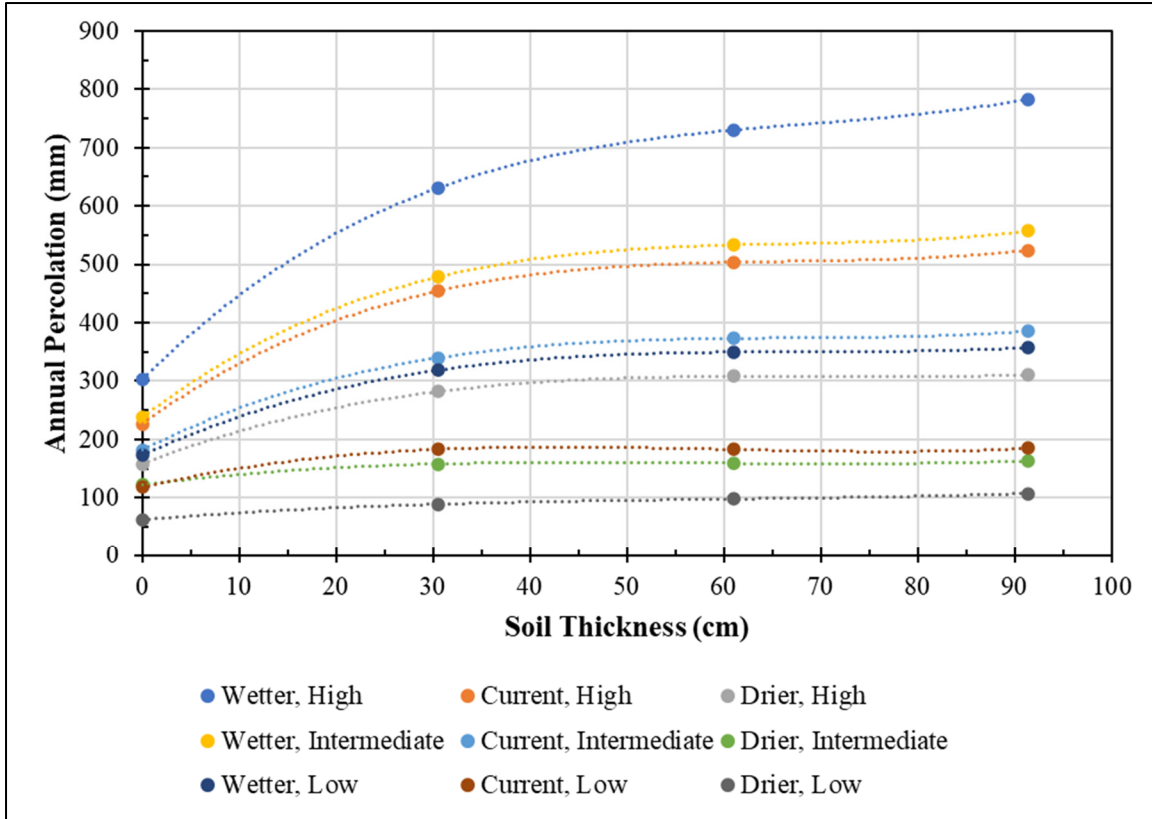


Fig. 5. Annual Percolation as a Function of Soil Thickness Above the Erosion Barrier.

The trendlines in Figure 5 are based on third-degree polynomial line-fits for each of the nine precipitation values used. As third-degree polynomial line fits, the respective percolations be estimated as a function of the soil thickness above the erosion barrier via:

$$q_p = ax^3 + bx^2 + cx + d \quad (\text{Eq. 1})$$

where

$q_p$  = the estimated annual percolation in (mm) for a specific precipitation ( $P$ ) value,  
 $x$  = the thickness of the soil above the erosion barrier (in cm),  
 $a$  = the first unitless polynomial coefficient (for application to  $x^3$ ),  
 $b$  = the second unitless polynomial coefficient (for application to  $x^2$ ),  
 $c$  = the third unitless polynomial coefficient (for application to  $x$ ), and  
 $d$  = the fourth unitless polynomial coefficient.

Each of the polynomial line fits were determined to have perfect one-to-one correlations ( $R^2 = 1$ ) to the corresponding percolation results, indicating that this empirical formula may be used to estimate annual percolation in lieu of the percolation models.

This first regression analysis defined in Equation 1 estimated annual percolation as a function of the soil thickness above the erosion barrier and provided a set of four polynomial coefficients. An additional regression analysis was then performed on each of the polynomial coefficients in Equation 1 to estimate annual percolation as a function of annual precipitation. This second regression analysis was actually performed four times, where each regression was used to estimate one of the four coefficient values ( $a$ ,  $b$ ,  $c$ , or  $d$ ) from Equation 1 as a function of annual precipitation.

In this step, different line-fitting distributions were tested (e.g., logarithmic, power law, etc.); however, perfect one-to-one correlations ( $R^2 = 1$ ) were not achieved. Regardless, it was determined that a second-degree polynomial line-fit could be applied to all four of the polynomial coefficients to provide very good line-fits (the resulting  $R^2$  values were 0.98 or better). The dotted lines in Figure 6 show each of the regression curves based on these second-degree polynomial line fits. Note that the  $b$  coefficients from Equation 1 are negative values; because negative values cannot be displayed on a logarithmic scale, the  $b$  coefficients in Figure 6 have been multiplied by -1 for display purposes.

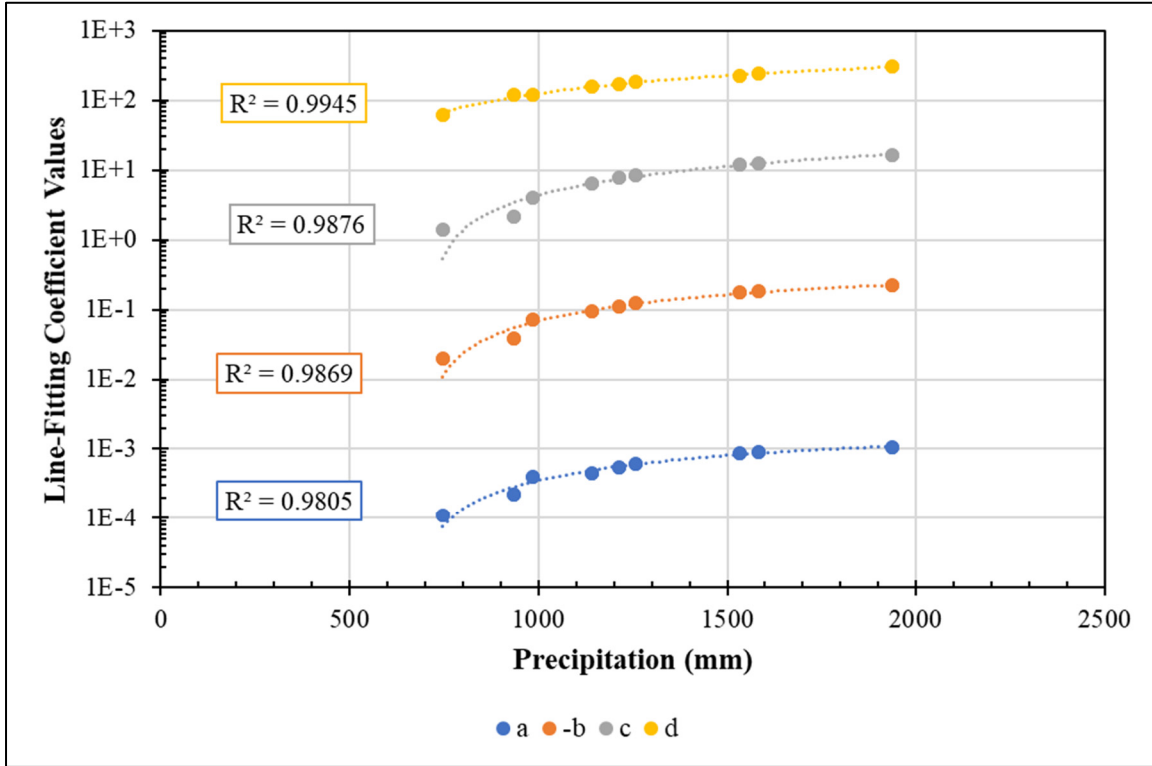


Fig. 6. Soil Thickness-to-Percolation Line Fitting Coefficients as a Function of Precipitation.

As second-degree polynomial line-fits, each of the soil thickness-to-percolation line-fitting coefficients from Equation 1 may be estimated via:

$$\phi_P = a_\phi P^2 + b_\phi P + c_\phi \quad (\text{Eq. 2})$$

where

- $\phi_P$  = the polynomial coefficient estimated for a specific annual precipitation ( $P$ ), where the polynomial coefficients are  $a$ ,  $b$ ,  $c$ , or  $d$  as determined from the trendlines in Figure 6,
- $P$  = the annual precipitation (in mm),
- $a_\phi$  = the first unitless polynomial coefficient (for application to  $P^2$ ),
- $b_\phi$  = the second unitless polynomial coefficient (for application to  $P$ ), and
- $c_\phi$  = the third unitless polynomial coefficient.

As with Equation 1, this formula is also an empirical formula, so the values must be input using the specified units (where applicable). Combining Equation 1 and Equation 2, and applying the corresponding values for each of the coefficients ( $a_\phi$ ,  $b_\phi$ , and  $c_\phi$ ), annual percolation (in mm) may be estimated as a function of both annual precipitation (in units of mm) and soil thicknesses above the

erosion barrier (in units of cm):

$$q_{P,x} = [(-2.562\text{E-}10P^2 + 1.550\text{E-}06P - 9.388\text{E-}04)x^3] \quad (\text{Eq. 3})$$

$$+ [(5.295\text{E-}08P^2 - 3.230\text{E-}04P + 2.010\text{E-}01)x^2]$$

$$+ [(-1.732\text{E-}06P^2 + 1.826\text{E-}02P - 1.213\text{E+}01)x]$$

$$+ [(-3.573\text{E-}05P^2 + 2.909\text{E-}01P - 1.294\text{E+}02)]$$

where

$q_{P,x}$  = the annual percolation (mm) for any given precipitation or soil thickness,

$P$  = the annual precipitation (mm), and

$x$  = the thickness of the soil above the erosion barrier (cm).

This empirical formula (Equation 3) provides an efficient approach for estimating annual percolation through the upper layers of the SDF closure cap when annual precipitation and erosion thicknesses are variable or change over time. Figure 7 compares the percolation model results from Table III against the equivalent percolation estimates based on Equation 3. This comparison shows that this approach for estimating annual percolation provides estimates that are nearly identical to those from the more complex Percolation Model. Based on this analysis, Equation 3 was applied to a fully probabilistic SDF closure cap model that was developed to support the response to RSI-1. [8]

Note that Equation 3 is based on the conceptual design of the SDF closure cap and assumed material properties and environmental conditions at the SDF. While Equation 3 may be used for equivalent simulations where the conditions and closure cap designs are similar, this formula is not valid for any other uses.

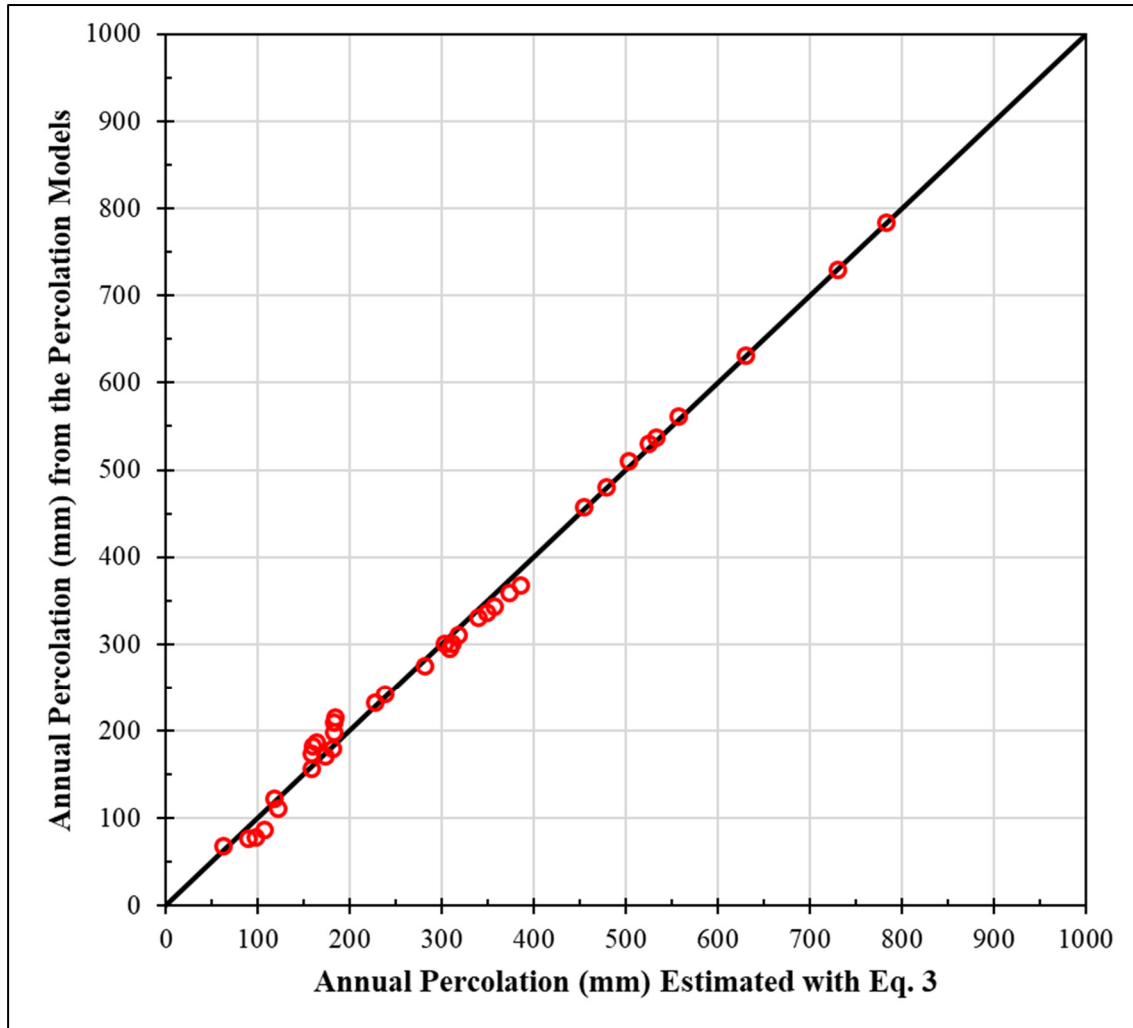


Fig. 7. Comparison of Percolation Estimates from the Percolation Model versus Percolation Estimates from Equation 3.

## CONCLUSIONS

Complex models are typically considered the preferred approach for modeling because intermediate values and formulas may be interrogated to improve understanding of system performance. However, these complex models can often be restrictive in their application or inefficient with respect to the time necessary to run the models. By using regression analyses to evaluate model results from a limited set of complex models, simplified empirical formulas may be developed. These empirical formulas may be applied to other models to expand functionality and can be used to reduce demand for computational resources.

The key to this approach is in identifying which inputs (or independent variables) have the greatest influence over specific model results (or dependent variables) so that appropriate parameters may be selected for performing the regression analyses. For example, the percolation results from the SDF Percolation Model were dependent on precipitation and erosional depth. Then, regression analyses can be performed on these key inputs to develop quantitative formulas that simplify the complex models into more efficient empirical formulas.

Using the empirical formula in Equation 3 allowed for the development of a fully probabilistic SDF closure cap model that integrated multiple variables and supported additional analyses of uncertainties associated with the long-term performance of the SDF closure system.

## REFERENCES

1. SRR-LWP-2009-00001, Chew, D.P., Hamm, B.A., and Wells, M.N., *Liquid Waste System Plan*, Savannah River Site, Aiken, SC, Rev. 22, September 2021.
2. SRR-CWDA-2020-00081, Arnett, B.E., *Determination of the SDF Inventory through 9/30/2020*, Savannah River Site, Aiken, SC, Rev. 0, December 2020.
3. SRR-CWDA-2020-00005, *Closure Plan for the Z-Area Saltstone Disposal Facility*, Savannah River Remediation, Aiken, SC, Rev. 1, August 2020.
4. SRR-CWDA-2019-00001, *Performance Assessment for the Saltstone Disposal Facility at the Savannah River Site*, Savannah River Site, Aiken, SC, Rev. 0, March 2020.
5. DOE M 435.1-1, Chg. 3, *Radioactive Waste Management Manual*, U.S. Department of Energy, Washington, DC, January 2021.
6. ML20254A003, Koenick, S. S., *Preliminary Review of the U.S. Department of Energy's Submittal of the 2020 Savannah River Site Saltstone Disposal Facility Performance Assessment*, U.S. Nuclear Regulatory Commission, Washington DC, October 2020.
7. SRR-CWDA-2021-00068, Hommel, S.P., *Summary of RSI Response Documents for the SDF PA*, Savannah River Site, Aiken, SC, Rev. 0, August 2021.
8. SRR-CWDA-2021-00040, Hommel, S.P., *Evaluation of the Uncertainties Associated with the SDF Closure Cap and Long-Term Infiltration Rates*, Savannah River Site, Aiken, SC, Rev. 0, June 2021.
9. WSRC-STI-2008-00244, Jones, W.E. and Phifer, M.A., *Saltstone Disposal Facility Closure Cap Concept and Infiltration Estimates*, Washington Savannah River Company, Aiken, SC, Rev. 0, May 2008.
10. SRR-CWDA-2018-00087, *Saltstone Disposal Facility Closure Cap Concept Update for Large-Scale Disposal Units*, Savannah River Remediation, Aiken, SC, Rev. 1, April 2019.
11. SCDHEC R.61-107.19, *SWM: Solid Waste Landfills and Structural Fill*, South Carolina Department of Health and Environmental Control, Columbia, SC, May 2008.
12. SRR-CWDA-2021-00031, Hommel, S.P., *Closure Cap Model Parameter Evaluation: Saturated Hydraulic Conductivity of Sand*, Savannah River Site, Aiken, SC, Rev. 1, May 2021.
13. SRR-CWDA-2021-00033, Hommel, S.P., *Closure Cap Model Parameter Evaluation: High Density Polyethylene (HDPE) and Geosynthetic Clay Liner (GCL) Composite Barrier Performance*, Savannah River Site, Aiken, SC, Rev. 1, May 2021.
14. SRR-CWDA-2021-00036, Hommel, S.P., *Evaluation of the Potential for Erosion in the Vicinity of Z Area*, Savannah River Site, Aiken, SC, Rev. 0, June 2021.
15. USDA-HDBK-703, Renard, K.G., Foster, G.R., Weesies, G.A., McCool, D.K., and Yoder, D.C.,



*Predicting Soil Erosion by Water: A Guide to Conservation Planning With the Revised Universal Soil Loss Equation (RUSLE)*, Agriculture Handbook Number 703, United States Department of Agriculture, Washington, DC, January 1997.

16. SRR-CWDA-2021-00081, Hommel, S.P., *Review of the Evapotranspiration Estimates Associated with Saltstone Disposal Facility Closure Cap Modeling*, Savannah River Site, Aiken, SC, Rev. 0, September 2021.